DRIVERS OF ELEVATED CHLOROPHYLL-A IN LUMAJANG WATERS: A COMPARATIVE ANALYSIS OF UPWELLING AND TERRESTRIAL RUNOFF MECHANISMS

***Bayu MUNANDAR*[1,3*], *Adzkia Noerma ARIFA*[1,2], *Annisa Aulia LUKMAN*[1], *Anindya WIRASATRIYA*[1] & *Yusuf Jati WIJAYA*[1]**

DOI: 10.21163/GT_2026.211.14

ABSTRACT

The Lumajang Waters (LW) is located in South Java and is one of the waters with outstanding primary productivity. The variation in primary productivity in a water body serves as an indicator of its aquatic fertility. Many seasonal parameters and physical oceanographic phenomena (currents, upwelling, nutrients, wind and waves) can influence the variability of chl-a in the ocean. In the current study, we conducted a comprehensive analysis of chl-a variability using both horizontal and vertical data. We found the highest chl-a in Lumajang waters occurred from July to October, and the El Niño Southern Oscillation (ENSO) and the Indian Ocean Dipole (IOD) events make higher chl-a. The peak chl-a concentration in 2019 was 2.03 mg/m³ in July, whereas in 2023 it reached 3.01 mg/m³ in October. However, we found the value of correlation between wind (Ekman Mass Transport (EMT)) and Chl-a was stronger in 2019 than in 2023. The coastal upwelling that increases in chl-a concentration in 2019 and 2023 is observable as a lifted water mass with a density of 23 kg/m³ from 100 meters depth to the surface. Despite lower intensity of coastal upwelling, chl-a concentration in 2023 was higher than in 2019. On the other hand, Rrs 555 in 2023 which represents Total Suspended Solids (TSS) exhibited a 2-times higher than the other years, particularly from August to October. The high Rrs 555 may be associated with the increase of TSS brought by river runoff, considering that many rivers flow from the upper land and fertilize the waters of Lumajang. These characteristics make Lumajang waters very unique, as two mechanisms run together influencing the chl-a variation.

Keywords: *Rrs 555; Upwelling; Chlorophyll-a; Density; Lumajang Waters.*

1. INTRODUCTION

The Lumajang Waters (LW) is located in South Java and is one of the waters that has outstanding primary productivity. This primary productivity is influenced by the location of the LW, which has a compact bathymetry and is passed by the South Java Current and the exit of the Indonesian Throughflow (Krabbenhoeft *et al*., 2010; Wijaya *et al.,* 2023; Guo *et al*., 2023; Sartimbul et al., 2023). This complexity creates the phenomena of oceanographic physics and the interaction of the atmosphere and the ocean. Rachman *et al.* (2024) stated that in the waters off southern Java, a coastal upwelling phenomenon occurs, which contributes to the variability of primary productivity in this region. The variation in primary productivity in a water body serves as an indicator of its aquatic fertility. The clean primary productivity in the form of plankton is an important element in the food chain of a body of water (Sarker *et al.,* 2023).

[1]*Oceanography, Faculty of Fisheries and Marine Sciences, Diponegoro University.* [*]*Corresponding author: (BM) bymunandar@gmail.com; (ANA) adzkia@lecturer.undip.ac.id; (AAL) aulialukman@lecturer.undip.ac.id; (AW) anindyawirasatriya@lecturer.undip.ac.id; (YJW) yusuf.jatiwijaya@live.undip.ac.id.*

[2] *Marine Science, Faculty of Fisheries and Marine Sciences, Diponegoro University.*

[3]*Technology and Business of Fisheries and Marine, Faculty of Fisheries and Marine Sciences, Diponegoro University.*

The abundance of phytoplankton can be monitored using chlorophyll-a (chl-a) concentration (Garini *et al*., 2021). Chl-a is the dominant color pigment in phytoplankton (Yun *et al.,* 2019). Furthermore, the variability of chl-a in the ocean can be influenced by many seasonal parameters and phenomena, including currents (An et al., 2025), upwelling (Munandar et al., 2023; Wirasatriya et al., 2023), nutrients (Maslukah et al., 2023), wind (Zampollo et al., 2025), and waves (Liu et al., 2025).

According to earlier research, variability of chl-a in the southern Indonesian seas is influenced by local and global scales of oceanographic phenomena. The local scale, such as monsoon (Haryanto et al., 2021), and the global scale, such as the IOD (Kunarso et al., 2023; Rachman et al., 2024), ENSO (Wijaya et al., 2020; Hidayat et al., 2025), Kelvin waves (Xu et al., 2018; Wijaya et al., 2024), precipitation (Kim et al., 2014; Wirasatriya et al., 2021). The high variability of chl-a concentration is a central indicator of marine productivity and a basis for predicting potential fishing ground area. Furthermore, many studies have indicated that plentiful fishery production in the southern Indonesian seas occurs during the upwelling season (Pet-Soede et al., 1999; Syamsuddin et al., 2013; Nugroho et al., 2022).

Previously, numerous researchers have conducted studies on the influence of IOD and ENSO on the variability of chl-a concentration in Indonesian seas. Susanto et al. (2001) was one of the early studies to identify the impact of ENSO on chl-a in this region. Additionally, Iskandar et al. (2022) investigated the extreme positive Indian Ocean dipole in 2019 and its impact on Indonesia. Rachman et al. (2024) examined the influence of ENSO and IOD on upwelling variability in the southern Indonesian region. The results indicated that IOD and ENSO can cause South Java Island's sea surface temperature to drop and its chlorophyll-a to rise. However, these studies often lack comprehensive information (Rachman et al., 2024; Iskandar et al., 2022; Susanto et al., 2001), which only analyzed the impact of IOD and ENSO on chl-a concentration in surface water and did not provide comprehensive vertical profile information to influence chl-a in surface water. Therefore, it is essential to conduct a more comprehensive analysis of the relationship between surface and vertical profile phenomena and the variation of chl-a. Further, we need to investigate the impact of EMT, TSS, IOD, and ENSO on these phenomena. Therefore, this study can provide more comprehensive insights into surface and vertical phenomena of chl-a and its connection to global phenomena. This research will establish a crucial scientific foundation for ocean management, with immediate implications for the prediction of fishery yields, the issuance of early warnings for harmful algal blooms, and the evaluation of the effects of climate change on marine ecosystems.

2. STUDY AREA

This research was carried out in the LW with coordinates of 7º S to 10º S and 111.5º E to 114.5º E (**Fig. 1**). This area is known to have a high upwelling due to strong wind, complex bathymetry and topography. We analyze the coastal and marine areas represented by the box in **Fig. 1**.

3. DATA AND METHODS

3.1. Data

To identify the variability of chl-a, we used data derived from the Ocean Colour Climate Change Initiative (OC-CCI), which is a program from the European Space Agency (ESA). OC-CCI are compelling from more than one satellite image with the high atmospheric correction and chl-a algorithm (Sathyendranath et al., 2019; Munandar et al., 2023) with the Root-Mean-Square Deviation (RMSD) reaches 0.34 (Garnesson et al., 2022) (OCEANCOLOUR_GLO_BGC_L4_MY_009_104). We used daily level 4 data with 0.04º spatial resolution interpolated to fill in missing data values. To examine the possible corruptions of satellite chl-a observation by the muddy water, we used reflectance remote sensing at 555 (Rrs 555) (https://oceancolor.gsfc.nasa.gov/l3/).

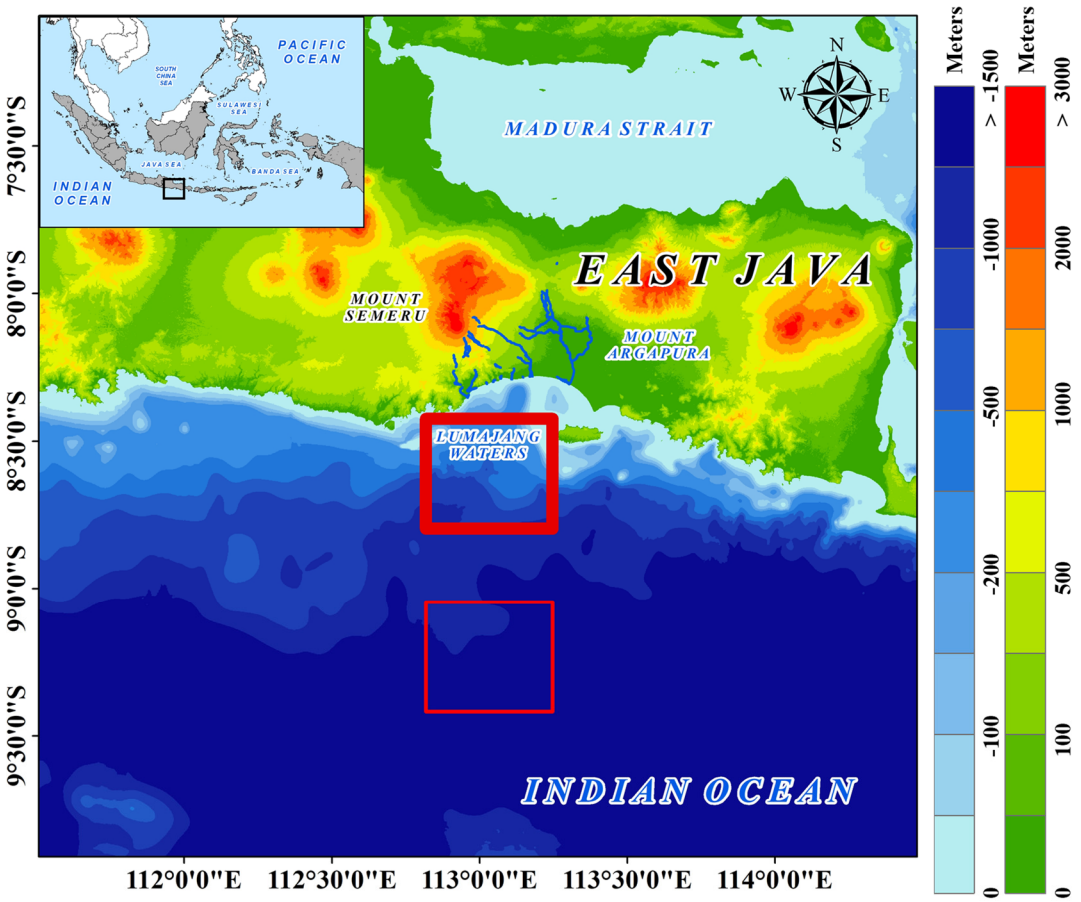

Fig. 1. Bathymetry and topography of the research area and names of the major seas. The thick and thin boxes depict the two area. The blue line is a river in Lumajang Regency.

To investigate the relationship between interannual phenomena and chl-a variability, we used IOD and ENSO. IOD and ENSO are calculated from the difference in anomaly of sea surface temperature in the Indian Ocean (IOD) and Pacific Ocean (ENSO). We obtained IOD data from https://stateoftheocean.osmc.noaa.gov/sur/ind/dmi.php#:~:text=The%20DMI%20index%20is%20an,Ocean%20Dipole%20or%20Zonal%20Mode. Next, ENSO data was obtained from https://origin.cpc.ncep.noaa.gov/products/analysis_monitoring/ensostuff/detrend.nino34.ascii.txt. The ONI data describes the value of the sea surface temperature anomaly (SSTA) found in the Niño 3.4 region. The frequencies of IOD and ENSO months during 2015–2024 are presented in **Fig. 2**.

To understand the vertical profile, we analyzed potential seawater density, which is calculated from seawater potential temperature and seawater salinity. The Copernicus Marine Environment Monitoring Service (CMEMS) (GLOBAL_MULTIYEAR_PHY_001_030) provides the temperature and salinity data. Both data have a spatial resolution of 0.083º × 0.083º, and the value of RMSD reaches 0.4ºC (temperature) and 0.2 psu (salinity). We obtained the precipitation data from ERA5 monthly averaged data on single levels (https://cds.climate.copernicus.eu) and this data has good accuracy (Jiao et al., 2021).

For wind and EMT analysis, the wind data can be accessed at https://www.remss.com/measurements/ccmp/. The data is combined with satellite data, mooring buoys, and model wind data (Mears et al., 2019). CCMP provides a spatial resolution of 0.25º×0.25º and an observation interval of 6 hours and the value of RMSE reaches 0.5 m/s (Atlas et al., 2011).

Next, the wind data is then further analyzed to obtain the EMT value. Bathymetry and topography were obtained from the Geospatial Information Agency of the Republic of Indonesia (https://tanahair.indonesia.go.id/). The observation period in this research is from January 2015 to December 2024. All the data will be calculated in each extreme phenomenon condition. Moreover, the satellite and reanalysis data have passed many quality checks and preprocessing procedures by the data source.

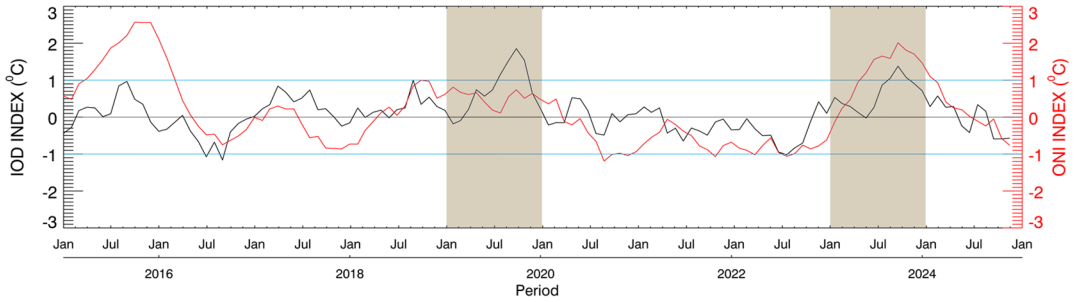

Fig. 2. Time series of the IOD and ENSO years from 2015–2024 based on the ONI 3.4 and DMI.

3.2. Method

Some of the data are daily time series data, so they need to be combined into monthly climatological data. The calculation of the monthly climatology follows the following equation:

$$\bar{X}(x,y) = \frac{1}{n}\sum_{i=1}^{n} x_i(x,y,t) \quad (1)$$

where $\bar{X}(x,y)$ is an average of the pixels data, $x_i(x,y,t)$ is the ith value of the data at position (x, y) and time (t). Further, n is a number of data (i.e., from 2015-2024). x_i is excluded from the calculation if that pixel has a missing data value. To investigate the EMT, first, we converted surface wind data into wind stress (τ) by using the following equation:

$$\tau = \rho_a C_d U_{10}^2 \quad (2)$$

where ρ_a is the density of air (1.25 kg m^3), Cd is the drag coefficient (WAMDI group, 1988) and U_{10} is the wind speed 10 m above sea level. The value of Cd follows WAMDI (1988). Next, we calculated classical EMT by following equations (i.e. Wang and Tang, 2014):

$$1000C_d = 1.29 \quad \text{for } 0 \text{ m/s} < U_{10} < 7.5 \text{ m/s}$$
$$1000C_d = 0.8 + 0.0065U_{10} \quad \text{for } 7.5 \text{ m/s} < U_{10} < 50 \text{ m/s}$$

$$EMT = -\frac{\tau}{\rho_w f} \quad (3)$$

where ρ_w is the density of seawater (1.025 kg m^3) and f is the Coriolis parameter ($f = 2\Omega \sin\theta$) (Stewart, 2008; Antonini & Caldeira, 2021). We also calculated potential seawater density at the normal atmospheric pressure from the profiles of temperature and salinity by using the UNESCO's (2015) formula. We also calculate *Pearson correlation* (bivariate correlaation) to determine the dominant role to chl-a variability.

4. RESULTS AND DISCUSSIONS

4.1. Monthly Variation of Surface Layer

We analyzed the monthly chl-a, IOD, ENSO, surface wind, wind stress, precipitation, Rrs 555, and EMT along the LW region from January to December over the periods of each dataset. **Figure 2** displays the IOD and ENSO conditions from 2015 to 2024. The peak condition of IOD occurred in 2019 and 2023, shown by the positive extreme values of 1.85269 and 1.37728, which occurred in October. Further, the peak of ENSO conditions arose in August 2019 and August 2023, showing ENSO positive reaches of 0.74 and 2.01, respectively (**Fig. 2**). Therefore, the present study focuses on 2019 and 2023, as the impact of EMT, upwelling, Rrs 555, IOD positive extremes and ENSO on chl-a concentrations is robust in both years.

The mean of monthly and climatological chl-a concentrations provides an overview of the time series evolution and spatial distribution of chl-a concentration in LW (**Fig. 3**). As shown in **Fig. 3B**, the highest chl-a concentration in 2019 reached 2.03 mg/m³ (July) and in 2023 reached 3.01 mg/m³ (October). This shows IOD+ and the El Niño event in 2023 had a stonger influence on increasing chl-a compared to the extreme IOD+ and the ENSO normal event in 2019 (**Fig. 2**). The patterns of monthly chl-a variation in 2019 and 2023 differed from the climatological pattern which has the highest chlorophyll-a in September (2.4 mg/m³) (**Fig. 3B**). The results prove that climate variation (IOD and ENSO) affects the variability of chlorophyll-a in LW.

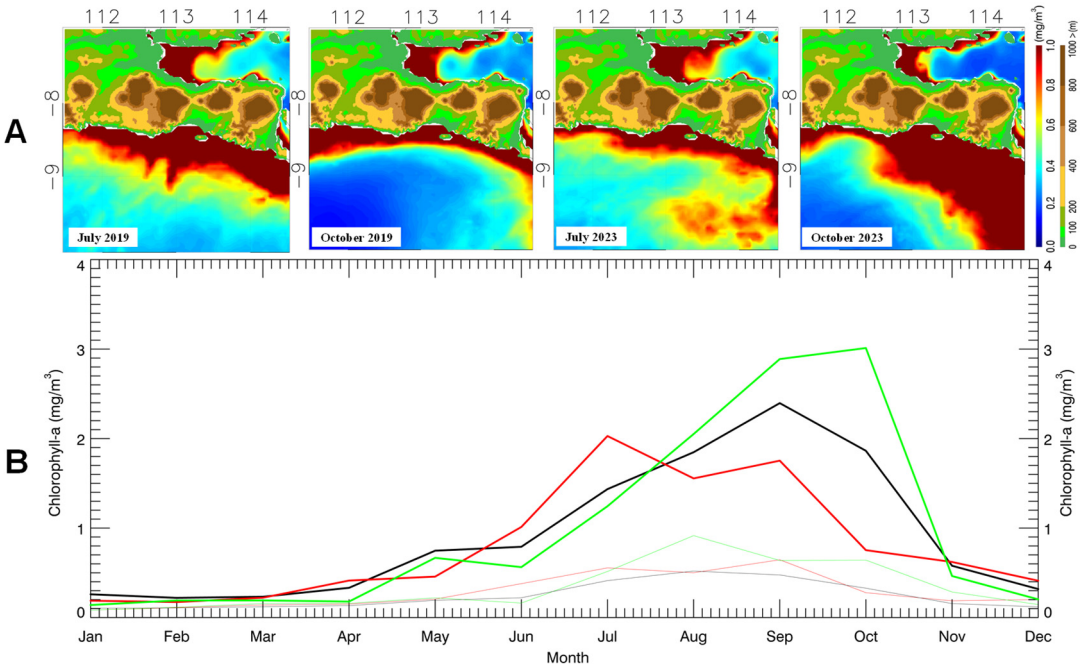

Fig. 3. The spatial distribution (A) and time series (B) variation of chl-a in LW and over the area 8.42º - 8.8º S, 112.82º - 113.24º E (thick box) and 9º - 9.42º S, 112.82º - 113.24º E (thin box). The thick box is represented onshore, and the thin box is shown offshore. The red line represents 2019, the green line shows 2023, and the black line shows climatology data. The peak of chl-a concentration in both areas is different from the peak of the same IOD and ENSO.

To investigate the variation of upwelling in 2019 and 2023, we calculated wind speed and EMT in this region. First, we generated the spatial distribution of wind speed and EMT (**Fig. 4**) and examined the relation with chl-a.

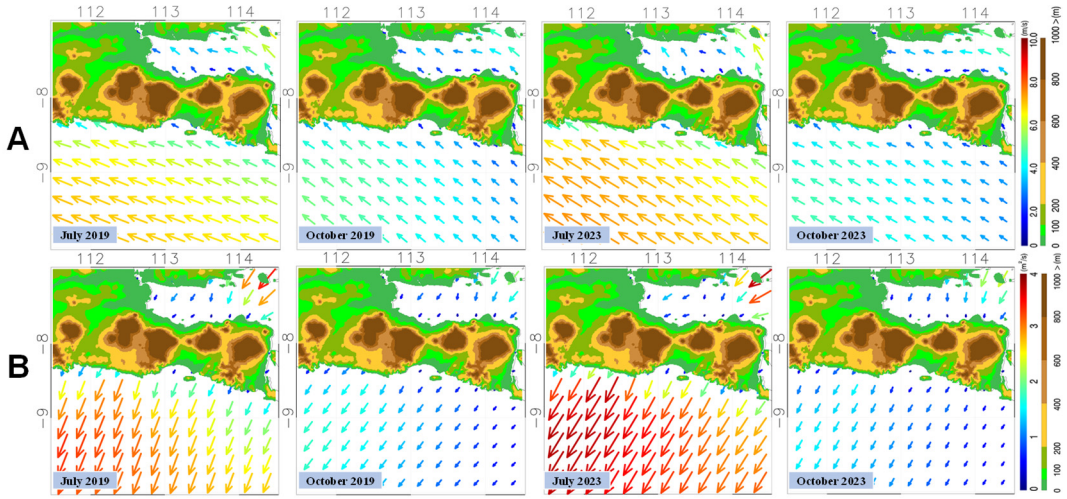

Fig. 4. Illustrates the spatial distribution of wind speed (A) and EMT (B) in LW. July and October represent peaks of IOD and ENSO events in 2019 and 2023.

Previous studies have confirmed that wind speed is a major physical factor that generatese the coastal upwelling process and then influences chl-a variability (Setiawan & Habibi, 2011; Wirasatriya et al., 2017; 2020; Kunarso et al., 2023; Munandar et al., 2023). **Figure 4** shows the distribution of wind speed and EMT in LW. In July and October, wind speed had the same direction to the northwest, with the highest speed occurring in February (8 m/s) and May (6.8 m/s) (**Fig. 5A**).

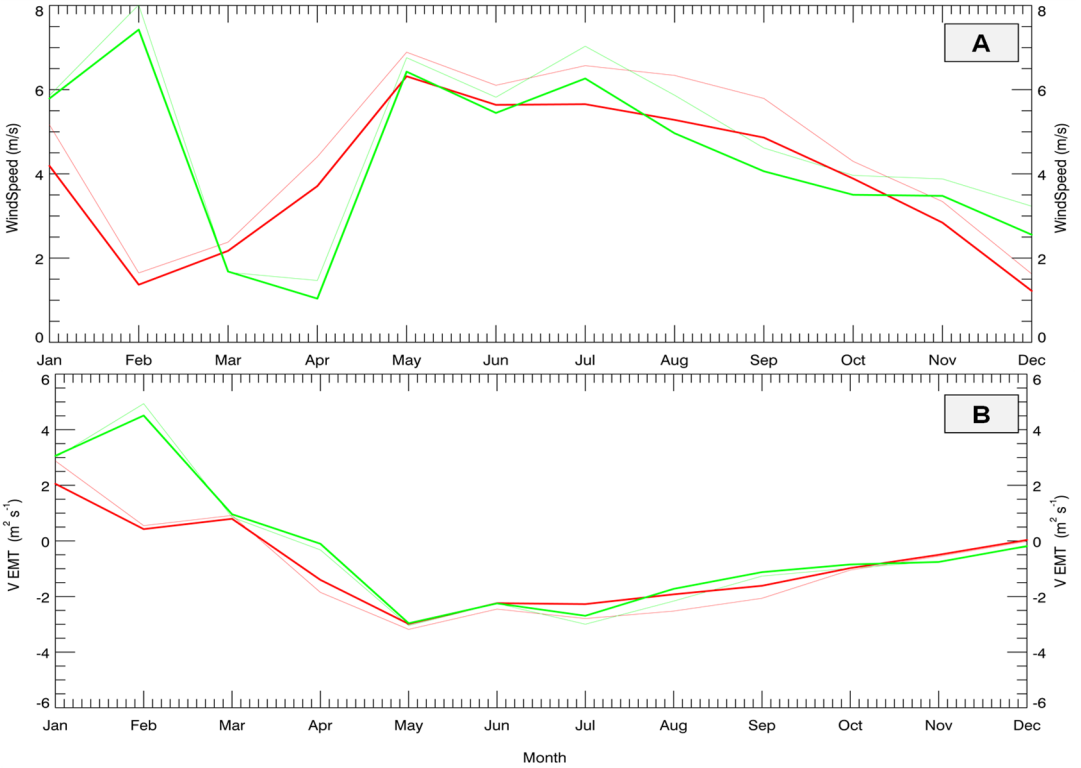

Fig. 5. Time series monthly of wind speed (A) and meridional EMT (B) in 2019 (red line) and 2023 (green line) (averaged from the thick box and thin box in Fig. 1). Negative (positive) meridional EMT means offshore (onshore) EMT.

The spatial and temporal data of wind speed revealed that the thick box (onshore) has lower wind speed compared with the thin box (offshore). Wirasatriya et al. (2019) demonstrated that the Coriolis effect may influence the impact of wind direction on EMT. The direction of the EMT is deflected clockwise in the northern hemisphere and counterclockwise in the southern hemisphere (Nouri et al., 2020). This is consistent with the EMT results obtained, where the wind direction in July and October is northwest, so that the direction of EMT is deflected counterclockwise to the southwest. The result of the EMT revealed that increased (decreased) offshore EMT occurred from May to December (from January to April) and the chl-a concentration was also higher from May to December than from January to April in both 2019 and 2020 (**Figs. 4B and 5B**). Wirasatriya et al. (2020) and Rachman et al. (2024) identified the steady southeast-to-northwest winds generate offshore EMT, which induces coastal upwelling and enhances chl-a concentrations.

4.2. Monthly Variation of Vertical Layer

The previous studies and analysis indicated coastal upwelling occurred, which explains the increased chl-a concentration in the surface layer (Rachman et al., 2024). The offshore EMT exhibited nearly the same value in 2019 and 2023. On the other hand, chl-a concentration in 2023 was higher than in 2019, with differences reaching up to 1 mg/m³ (**Fig. 3**). To prove that the increasing chl-a in 2019 and 2023 resulted from coastal upwelling, we calculated the vertical profile of potential seawater density from temperature and salinity data. We focused on the thick box (**Fig. 1**) due to its highest concentration of chl-a.

The lifting of higher-density water masses signified the occurrence of coastal upwelling in both years. The lifting isopycnal of 23 kg/m³ reached a surface of 10 m from June to November, indicating the coastal upwelling process in 2019 (**Fig. 6a**). In contrast, the lifting isopycnal of 23 kg/m³ reached a surface of 10 m from August to October indicates the coastal upwelling process in 2023. This observation is consistent with the findings of Wirasatriya et al. (2020) and Rachman et al. (2024), who reported that coastal upwelling in the south of Java occurs in the eastern season, marked by the occurrence of shoaling of pycnocline depth. Nevertheless, the result indicates that coastal upwelling in 2019 was stronger than in 2023, as denoted by the higher surface density (i.e., more than 22.5 kg/m³) from June to November.

In accordance with the previous studies (Wang & Tang, 2014; Wirasatriya et al., 2020; Munandar et al., 2023; Rachman et al., 2024; Xu et al., 2025), upwelling clearly had an impact on the higher chl-a concentration in 2019 in LW. On the opposite side, the highest chl-a in 2023 did not seem to have a clear effect of upwelling on the increasing chl-a concentrations in LW.

Furthermore, we conducted a statistical analysis to determine the association between chl-a, EMT, and wind speed for both years, as shown in **Table 1**. In 2019, the correlation between chl-a and meridional EMT was very significant (-0.62*), and the correlation between chl-a and wind speed was also very significant (0.6*). In contrast, the correlation between chl-a and meridional EMT in 2023 was lower (0.41), while no significant correlation was found between chl-a and wind speed in 2023 (0.03). These result suggest that meridional EMT (upwelling event) had a greater impact on chl-a variation in 2019 compared to 2023. Thereby, other phenomena likely contributed to the increase in chl-a concentration in LW in addition to upwelling in 2023. In the next section, we examine the possible mechanisms that explain why chl-a levels in 2023 was higher than those in 2019 in LW.

Table 1.
Highly significant correlation analysis ($p < 0.05$) among monthly chl-a, meridional EMT, and wind speed in Jan – Dec 2019 and Jan – Dec 2023 inside the thick boxes as shown in Fig. 1.

	Variable	Meridional EMT	Wind Speed
Chl-a	2019	-0.62*	0.6*
	2023	-0.41	0.03

** Correlation is significant at the 0.05 level (1-tailed).*

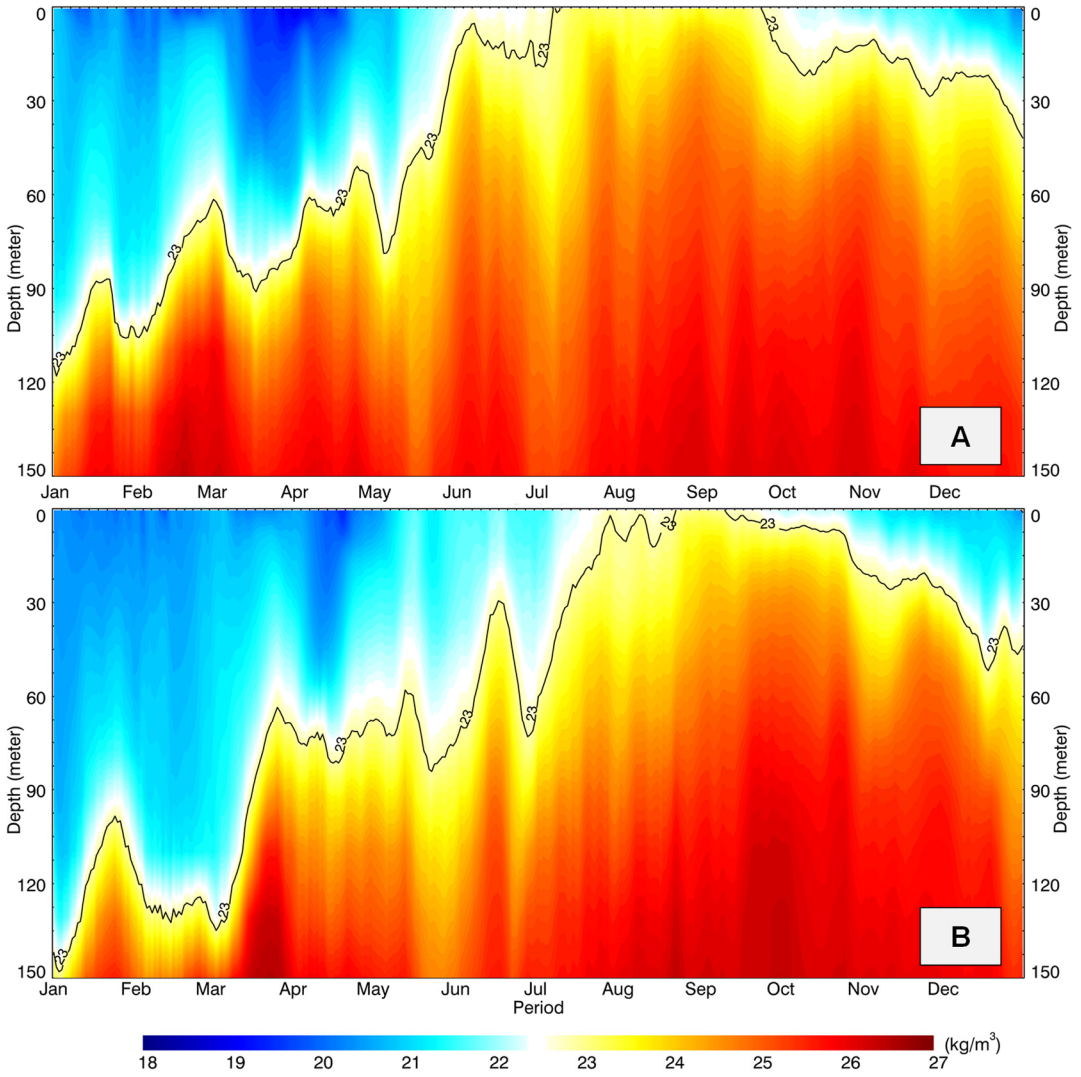

Fig. 6. Vertical profile of daily potential seawater density in Lumajang Waters in 2019 (A) and 2023 (B) (average from the thick box) using reanalysis data. The black contours in A) and B) are isopycnals of 23 kg/m³.

4.3. Possibility of Total Suspended Solids impact on chlorophyll-a

To investigate other possibilities for the mechanism to influence the highest chl-a, we analyzed time series precipitation and Rrs 555. To address the incongruity of the relationship between meridional EMT and Chl-a, we plot the temporal variability of precipitation and Chl-a in both years in **Fig. 7**. We expand the average precipitation area to the upland area to account for the potential impact of the river runoff during the rainy season. Wirasatriya et al. (2021) demonstrated the river runoff may increase the chl-a concentration; this rise is due to the existence of anthropogenic compounds.

September and October did not clearly show a significant increase in precipitation in the Lumajang area. Nevertheless, the topography of Lumajang Regency can affect river runoff. Lumajang Regency is surrounded by volcanoes (Mount Semeru and Mount Argopuro) and the ocean (Indian Ocean). Mount Semeru last erupted in 2023, while no eruptions occurred in 2019 (Handoko et al., 2025). The eruption of Mount Semeru was expected to increase the sediment influx into the LW rather than the precipitation.

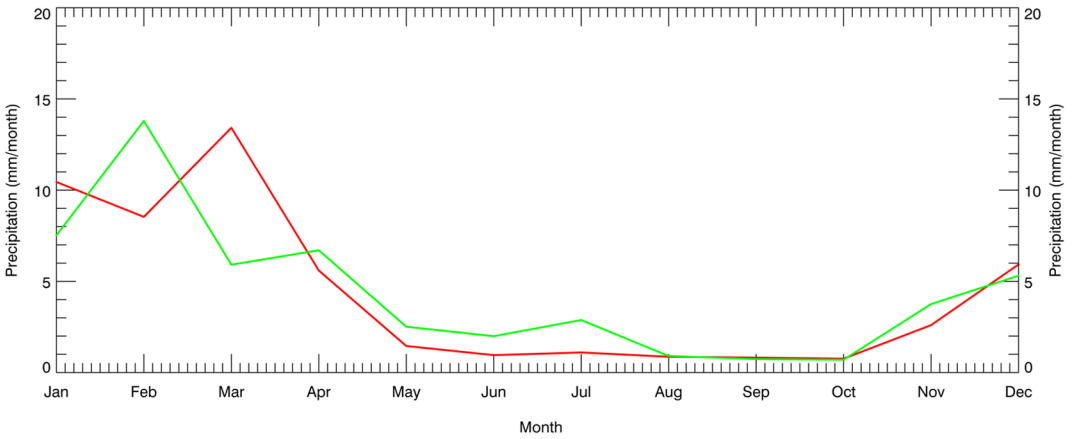

Fig. 7. Time series of monthly precipitation in 2019 (red line) and 2023 (green line) (averaged from the thick box in **Fig. 1**).

Furthermore, many rivers discharge into the Lumajang Waters (i.e., Bondoyudo River, Mujur River, Rakinten River and others). Volcanic material was probably transported from upper land to the sea through these rivers. The TSS from river runoff can influence the results of imagery from satellite observations (Maslukah et al., 2024). Volcanic ash or volcanic material (sediment) can also affect the variability of chl-a concentration in seawater (Katada et al., 2025). The apparent rise in chl-a concentrations may result from erroneous satellite image observations attributed to TSS.

To investigate the possibility of TSS influencing the error of the observations of chl-a concentration, we used Rrs 555 to identify TSS in the ocean. Many previous studies have used Rrs 555 for the identification of TSS, including Mobley et al. (2004); Siswanto et al. (2011); Matsushita et al. (2012); Wang & Tang (2014); Wirasatriya et al. (2021); Munandar et al. (2023); and Wijaya et al. (2024). According to Matsushita et al. (2012), the ocean is categorized into case-1 and case-2 waters. Case-1 waters are clean waters and have less contamination, while case-2 waters are more complex and contain more contaminat. The increase in Rrs 555 suggests that the chlorophyll-a measurements obtained from satellite images is inaccurate, as they represent a lot more than just phytoplankton. From 2015 to 2022 and in 2024, Rrs 555 was at most 0.0025 sr^{-1} throughout the year. In contrast, Rrs 555 in 2023 exhibited a 2-times higher than the other years, particulary from August to October (**Fig. 8**). To convince the influence of Rrs 555 to chl-a, we calculated the correlation between Rrs 555 and chl-a. In 2019 and 2023, the value of correlation between Rrs 555 and chl-a was categorized as high, However, it was higher in 2023 (0.83**), than in 2019 (0.53) (**Table 2**).

As discussed earlier, the TSS in 2019 is lower than that in 2023, but overall, the Lumajang Waters can be categorized as case-2 water. This condition may be attributed to the increase in river runoff, considering that many rivers flow into the waters of Lumajang and originate from the surrounding volcanoes. The precipitation data is not clearly seen to capture the increasing river runoff in Lumajang Waters, besides upwelling. Therefore, further in-situ observations of river runoff and TSS are needed to understand the TSS source in Lumajang waters. Consequently, the findings suggest that the anthropogenic activities in the upland area may contributed to the variability of chl-a concentration in Lumajang Waters.

Table 2.
Highly significant correlation analysis ($p < 0.01$) between monthly chl-a and Rrs 555 in Jan – Dec 2019 and Jan – Dec 2023 inside the thick boxes as shown in **Fig. 1.**

	Variable	Rrs 555
Chl-a	2019	0.53
	2023	0.83**

**. *Correlation is significant at the 0.01 level (1-tailed).*

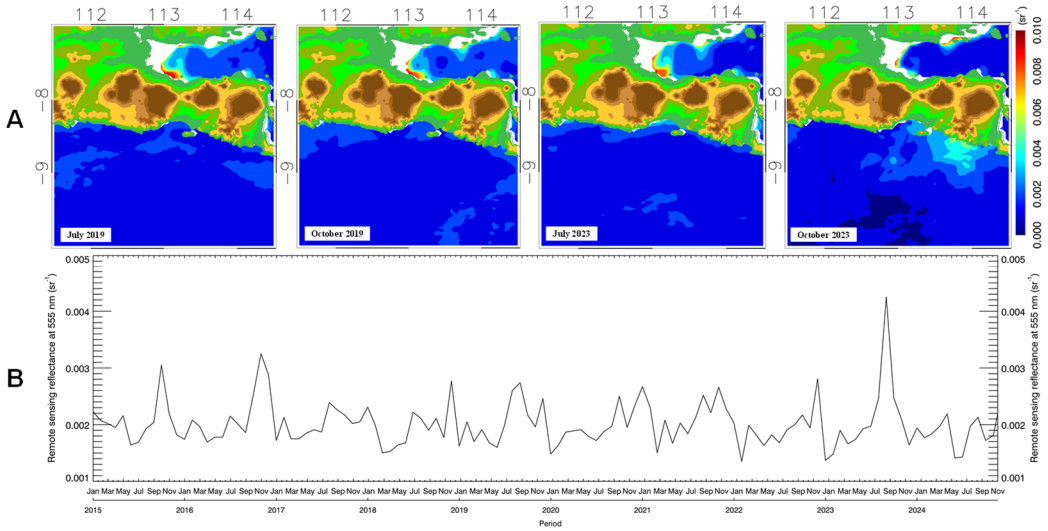

Fig. 8. The spatial distribution (A) and time series (B) variation of Rrs 555 in LW from 2015 to 2024 (averaged from the thick box in **Fig. 1**).

6. CONCLUSIONS

Blended satellite-based data provide effective means to investigate water parameters in Lumajang waters. Lumajang Waters have been identified as having the highest chl-a concentration, which occurred during the east monsoon and transition II seasons due to the coastal upwelling. The monthly chl-a variations in 2019 and 2023 ranges from 0.1 mg/m³ to 2 mg/m³ and 0.1 mg/m³ to 3 mg/m³, respectively. The coastal upwelling that increases in chl-a concentration in 2019 and 2023 is observable as a lifted water mass with a density of 23 kg/m³ from 100 meters depth to the surface. Despite lower intensity of coastal upwelling, chl-a concentration in 2023 was higher than in 2019. On the other hand, Rrs 555 in 2023 which represents TSS exhibited a 2-times higher than the other years, particularly from August to October. The high Rrs 555 may be associated with the increase of TSS brought by river runoff, considering that many rivers flow from the upper land and fertilize the waters of Lumajang. These characteristics make Lumajang waters very unique, as two mechanisms run together influencing the chl-a variation.

ACKNOWLEDGEMENT

This research was funded by the non-APBN DPA LPPM 2025, Universitas Diponegoro, under Contract No: 222-150/UN7.D2/PP/IV/2025, with Addendum No: 745/UN7.D2/PP/X/2025. The authors also extend their gratitude to the National Aeronautics and Space Administration (NASA) and the Copernicus Marine Environment Monitoring Service (CMEMS) and all related agencies for providing the satellite data that was essential for this study. Additionally, we appreciate the expertise of the anonymous reviewers who greatly enhanced the paper.

REFERENCES

An, L., Huang, Y., Xu, C., Xu, F., Chen, J., Liu, X. & Huang, B. 2025. Biogeochemical characteristics and phytoplankton community diversity of the Western North Equatorial current. *Global and Planetary Change,* 252, 104895. https://doi.org/10.1016/j.gloplacha.2025.104895.

Antonini, E.G.A. & Caldeira, K. 2021. Atmospheric pressure gradients and coriolis forces provide geophysical limits to power density of large wind farms. *Appl. Energy*, 281, 116048. https://doi.org/10.1016/j.apenergy.2020.116048.

Atlas, R., Hoffman, R. N., Ardizzone, J., Leidner, S. M., Jusem, J. C., Smith, D. K. & Gombos, D. 2011. A Cross-calibrated, Multiplatform Ocean Surface Wind Velocity Product for Meteorological and Oceanographic Applications. *Bulletin of the American Meteorological Society,* 92(2): 157–174. https://doi.org/10.1175/2010BAMS2946.1.

Garini, B. N., Suprijanto, J. & Pratikto, I. 2021. Chlorophyll-a Content and Abundance in The Waters of Kendal, Central Java. *Journal of Marine Research*, 10(1): 102-108. https://doi.org/10.14710/jmr.v10i1.28655.

Guo, Y., Li1, Y., Cheng, L., Chen, G., Liu, Q., Tian, Hu, S., Wang, J. & Wang, F. 2023. An Updated Estimate of the Indonesian Throughflow Geostrophic Transport: Interannual Variability and Salinity Effect. *Geophysical Research Letters*, 50, e2023GL103748. https://doi.org/10.1029/2023GL103748.

Garnesson, P., Mangin, A. & Bretagnon, M. 2022. OCEAN COLOUR PRODUCTION CENTRE Satellite Observation Copernicus-GlobColour Products. ⟨https://catalogue. marine.copernicus.eu/documents/QUID/CMEMS-OC-QUID-009–101to104–116-118.pdf.

Handoko, E. Y., Maulida, P. & Syaifullah, S. A. 2025. TheEffect of Semeru VolcanicEruption on Variatioin in Precipitation Water Vapor Using the GPS measurementin Period 2020–2023. *Jurnal Geosains dan Remote Sensing,* 6(1): 65-80. https://doi.org/10.23960/jgrs.ft.unila.356.

Haryanto, Y. D., Riama, N. F., Purnama, D. R., Pradit, N., Ismah, S. F., Suryo, A. W., Fadli, M., Hananto, N. D., Li, S. & Susanto, R. D. 2021. Effect of Monsoon Phenomenon on Sea Surface Temperatures in Indonesian Throughflow Region and Southeast Indian Ocean. *Journal of Southwest Jiaotong University*, 56(6): 914-923. https://doi.org/10.35741/issn.0258-2724.56.6.80.

Hidayat, M. N., Wafdan, R., Iskandar, T., Dewi, C. D., Nurhayati, N., Ramli, M., Muchlisin, Z. A. & Rizal, S. 2025. The influence of El Niño-Southern Oscillation and the Indian Ocean Dipole on chlorophyll-a in the Aceh waters during 1999–2023. *International Journal of Remote Sensing*, *46*(7): 2888–2908. https://doi.org/10.1080/01431161.2025.2460244.

Iskandar, I., Lestari, D. O., Saputra, A. D., Setiawan, R. Y., Wirasatriya, A., Susanto, R. D., Mardiansyah, W., Irfan, M., Rozirwan, Setiawan, J. D. & Kunarso. 2022. Extreme Positive Indian Ocean Dipole in 2019 and Its Impact on Indonesia. *Sustainability*, 14(22): 15155. https://doi.org/10.3390/su142215155.

Jiao, D., Xu, N., Yang, F. & Xu, K. 2021. Evaluation of spatial-temporal variation performance of ERA5 precipitation data in China. *Scientific Reports,* 11, 17956. https://doi.org/10.1038/s41598-021-97432-y.

Katada, R., Ariyoshi, S., Ayuzawa, H., Saito, K., Ishizaka, J. & Iwabuchi, H. 2025. Relation between eruption at Nishinoshima and chlorophyll-a concentration at Ogasawara Islands in 2020. *Progress in Earth and Planetary Science,* 12, 85. https://doi.org/10.1186/s40645-025-00761-z.

Kim, T., Najjar, R.G. & Lee, K. 2014. Influence of precipitation events on phytoplankton biomass in Coastal Waters of the Eastern United States. *Glob. Biogeochem. Cycles*, 28(1): 1–13. https://doi.org/10.1002/2013GB004712.

Krabbenhoeft, A., Weinrebe, R. W., Kopp, H., Flueh, E. R., Ladage, S., Papenberg, C., Planert, L. & Djajadihardja, Y. 2010. Bathymetry of the Indonesian Sunda margin-relating morphological features of the upper plate slopes to the location and extent of the seismogenic zone. *Natural Hazards and Earth System Sciences,* 10(9): 1899–1911. https://doi.org/10.5194/nhess-10-1899-2010.

Kunarso, Ismunarti, D. H., Rifai, A., Munandar, B., Wirasatriya, A. & Susanto, R. D. 2023. Effect of Extreme ENSO and IOD on the Variability of Chlorophyll-a and Sea Surface Temperature in the North and South of Central Java Province. *ILMU KELAUTAN: Indonesian Journal of Marine Sciences*, 28(1): 1-11. https://doi.org/10.14710/ik.ijms.28.1.1-11.

Liu, X., Pu, X., Qu, D. & Xu, Z. 2025. The role of wave-induced mixing in spring phytoplankton bloom in the South Yellow Sea. *Marine Pollution Bulletin,* 211, 117374. https://doi.org/10.1016/j.marpolbul.2024.117374.

Maslukah, L., Handoyo, G., Wulandari, S. Y., Sihite, C. B. & Sarjito. 2023. The Chlorophyll-a Response of Phytoplankton to Ratio N/P in Different Coastal Waters. *Ecological Engineering & Environmental Technology*, 24(9): 121–129. http://dx.doi.org/10.12912/27197050/172292.

Maslukah, L., Wirasatriya, A., Wijaya, Y. J., Ismunarti, D. H., Widiaratih, R. & Krisna, H. N. 2024. The assessment of chlorophyll-a retrieval algorithm and its spatial-temporal distribution using sentinel-2 MSI off the Banjir Kanal Timur River, Semarang, Indonesia. *Regional Studies in Marine Science*, 75. 103556. https://doi.org/10.1016/j.rsma.2024.103556.

Matsushita, B., Yang, W., Chang, P., Yang, F. & Fukushima, T. 2012. A simple method for distinguishing global case-1 and case-2 waters using SeaWiFS measurements. *ISPRS J. Photogramm. Remote Sens*. 69, 74–87. https://doi.org/10.1016/j.isprsjprs.2012.02.008.

Mears, C. A., Scott, J., Wentz, F. J., Ricciardulli, L., Leidner, S. M., Hoffman, R. & Atlas, R. 2019. A Near-Real-Time Version of the Cross-Calibrated Multiplatform (CCMP) Ocean Surface Wind Velocity Data Set. *Journal of Geophysical Research: Ocean,* 124(10): 6997-7010. https://doi.org/10.1029/2019JC015367.

Mobley, C.D., Stramski, D., Bissett, W. P. & Boss, E. 2004. Optical modeling of ocean waters: is the case 1 - case 2 classification still useful. *Oceanography*, 17 (2): 60–67. https://doi.org/10.5670/oceanog.2004.48.

Munandar, B., Wirasatriya, A., Sugianto, D. N., Susanto, R. D., Purwandana, A. & Kunarso. 2023. Distinct mechanisms of chlorophyll-a blooms occur in the Northern Maluku Sea and Sulu Sill revealed by satellite data. *Dynamics of Atmospheres and Oceans,* 102, 101360. https://doi.org/10.1016/j.dynatmoce.2023.101360.

Nouri, R., Vasel-Be-Hagh, A. & Archer, C. L. 2020. The Coriolis force and the direction of rotation of the blades significantly affect the wake of wind turbines. *Applied Energy,* 277. 115511. https://doi.org/10.1016/j.apenergy.2020.115511.

Nugroho, S. C., Setiawan, R. Y., Setiawati, M. D., Djumanto, Priyono, S. B., Susanto, R. D., Wirasatriya, A. & Larasati, R. F. 2022. Estimation of Albacore Tuna Potential Fishing Grounds in the Southeastern Indian Ocean. *IEEE Access,* 11: 1141 – 1147. https://doi.org/10.1109/ACCESS.2022.3233353.

Pet-Soede, C., Cesar, H. S. J. & Pet, J. S. 1999. An Economic Isuues Related to Blast Fishing on Indonesia Coral Reefs. *Enviromental Conservation*, 26(2): 83-93. https://doi.org/10.1017/S0376892999000132.

Rachman, H. A., Setiawati, M. D., Hidayah, Z., Syah, A. F., Nandika, M. R., Lumban-Gaol, J., As-syakur, A. R. & Syamsudin, F. 2024. Dynamic of upwelling variability in southern Indonesia region revealed from satellite data: Role of ENSO and IOD. *Journal of Sea Research,* 202: 102543. https://doi.org/10.1016/j.seares.2024.102543.

Sarker, S., Hossain, M. S., Sonia, M. I., Huda, A. N. M. S., Riya, S. C., Das, N., Liyana, E., Basak, S. C. & Kabir, M. A. 2023. Predicting the impacts of environmental variability on phytoplankton communities of a sub-tropical estuary. *Journal of Sea Research*, 194. 102404. https://doi.org/10.1016/j.seares.2023.102404.

Sartimbul, A., Winata, V.A. Kasitowati, R.D., Iranawati, F., Rohadi, E., Yona, D., Anjeli, U.G., Pranowo, W.S. & Lauro, F. M. 2023. Seasonal Indonesian Throughflow (ITF) across southern Java determines genetic connectivity of Sardinella lemuru (Bleeker, 1835). *Deep-Sea Research Part II,* 209, 105295. https://doi.org/10.1016/j.dsr2.2023.105295.

Sathyendranath, S., Brewin, R. J. W., Brockmann, C., Brotas, V., Calton, B., Chuprin, A., Cipollini, P., Couto, A.B., Dingle, J., Doerffer, R., Donlon, C., Dowell, M., Farman, A., Grant, M., Groom, S., Horseman, A., Jackson, T., Krasemann, H., Lavender, S., Martinez-Vicente, V., Mazeran, C., M´elin, F., Moore, T.S., Müller, D., Regner, P., Roy, S., Steele, C.J., Steinmetz, F., Swinton, J., Taberner, M., Thompson, A., Valente, A., Zühlke, M., Brando, V.E., Feng, H., Feldman, G., Franz, B.A., Frouin, R., Gould Jr, R.W., Hooker, S.B., Kahru, M., Kratzer, S., Mitchell, B.G., Muller-Karger, F.E., Sosik, H.M., Voss, K.J., Werdell, J. & Platt, T. 2019. An oceancolour time series for use in climate studies: the experience of the ocean-colour climate change initiative (OC-CCI). *Sensors*, 19(19), 4285. https://doi.org/10.3390/s19194285.

Setiawan, R.Y. & Habibi, A. 2011. Satellite detection of summer chlorophyll-a bloom in the Gulf of Tomini. IEEE J. Sel. Top. Appl. Earth Obs. *Remote Sens*., 4(4): 944–948. https://doi.org/10.1109/JSTARS.2011.2163926.

Siswanto, E., Tang, J., Yamaguchi, H., Ahn, Y., Ishizaka, J., Yoo, S., Kim, S., Kiyomoto, Y., Yamada, K., Chiang, C. & Kawamura, H. 2011. Empirical ocean-color algorithms to retrieve chlorophyll-a, total suspended matter, and colored dissolved organic matter absorption coefficient in the Yellow and East China Seas. *J. Oceanogr.* 67, 627–650. https://doi.org/10.1007/s10872-011-0062-z.

Susanto, R. D., Gordon, A. L. & Zheng, Q. 2001. Upwelling along the coasts of Java and Sumatra and its relation to ENSO. *Geophysical Research Letters,* 28(8): 1599-1602. https://doi.org/10.1029/2000GL011844.

Syamsuddin, M. L., Saitoh, S., Hirawake, T., Bachri, S. & Harto, A. B. 2013. Effects of El Niño–Southern Oscillation eventson catches of Bigeye Tuna (Thunnus obesus) inthe eastern Indian Ocean off Java. *Fishery Bulletin,* 111(2): 175-188. https://doi.org/10.7755/FB.111.2.5.

UNESCO, 2015. Tenth Report of the Joint Panel on Oceanographic Tables and Standards. UNESCO Technical Papers in Marine Science. Paris. 25p.

Wang, J.J. & Tang, D.L. 2014. Phytoplankton patchiness during spring intermonsoon in Western Coast of South China Sea. *Deep-Sea Res. II,* 101: 120–128. https://doi.org/10.1016/j.dsr2.2013.09.020.

WAMDI group. 1988. The WAM model: a third-generation ocean wave prediction model. *J. Phys. Oceanogr.*, 18 (12): 1775–1810. https://doi.org/10.1175/1520-0485(1988)018<1775:TWMTGO>2.0.CO;2.

Wijaya, A., Zakiyah, U., Sambah, A. B. & Setyohadi, D. 2020. Spatio-temporal variability of temperature and chlorophyll-a concentration of sea surface in Bali Strait, Indonesia. *Biodiversitas,* 21(11): 5283-5290. https://doi.org/10.13057/biodiv/d211132.

Wijaya, Y. J., Wisha, U. J., Rejeki, H. A. & Ismunarti, D. H. 2023. Variability of the South Java Current from 1993 to 2021, and its relationship to ENSO and IOD events. *Asia-Pacific Journal of the Atmospheric Sciences,* 60(17): 15. http://dx.doi.org/10.1007/s13143-023-00336-2.

Wijaya, Y. J., Wisha, U. J., Maslukah, L. Windarto, S., Wirasatriya, A. & Zainuri, M. 2024. Seasonal variation of chlorophyll-a in South Java over the past quarter-century. *Ocean Dynamics,* 74: 703–724. https://doi.org/10.1007/s10236-024-01629-4.

Wirasatriya, A., Setiawan, R.Y. & Subardjo, P. 2017. The effect of ENSO on the variability of chlorophyll-a and sea surface temperature in the Maluku Sea. *IEEE J. Sel. Top. Appl. Earth Obs. Remote Sens*., 10(12): 5513–5518. https://doi.org/10.1109/JSTARS.2017.2745207.

Wirasatriya, A., Sugianto, D.N., Helmi, M., Setiawan, R.Y. & Koch, M. 2019. Distinct characteristics of SST variabilities in the Sulawesi Sea and the Northern Part of the Maluku Sea during the southeast monsoon. *IEEE J. Sel. Top. Appl. Earth Obs. Remote Sens*., 12 (6): 1763–1770. https://doi.org/10.1109/JSTARS.2019.2913739.

Wirasatriya, A., Susanto, R.D., Setiawan, J. D., Ramdani, F., Iskandar, I., Jalil, A. R., Puryajati, A. D., Kunarso & Maslukah, L. 2021. High Chlorophyll-a Areas along the Western Coast of South Sulawesi-Indonesia during the Rainy Season Revealed by Satellite Data. *Remote Sens.,* 13, 4833. https://doi.org/10.3390/rs13234833.

Wirasatriya, A., Susanto, R. D., Setiawan, J. D., Agustiadi, T., Iskandar, I., Ismanto, A., Nugraha, A. L., Puryajati, A. D., Kunarso, Purwandana, A., Ramdani, F., Lestari, T. A., Maro, J. F., Kitarake, Y. N. S., Sailana, Y. L., Goro, M. S., Hidayah, B. K., Widiaratih, R., Fitria, S. & Dollu, E. A. 2023. Extreme Upwelling Events in the Seas of the Alor Kecil, Alor Island, Indonesia. *Oceanography,* 36(1): 28 – 37. https://doi.org/10.5670/oceanog.2023.107.

Xu, Y., Li, S., Hamzah, F., Setiawan, A., Susanto, R. D., Cao, G. & Wei, Z. 2018. Intraseasonal flow and its impact on the chlorophyll-a concentration in the Sunda Strait and its vicinity. *Deep-Sea Research Part I*, 136: 84-90. https://doi.org/10.1016/j.dsr.2018.04.003.

Xu, Wang, D., Wei, Q., Li, S., Susanto, R. D., Wang, G., Teng, F., Agustiadi, T., Trenggono, M., Santoso, P. D. & Wei, Z. 2025. Satellite-detected Sea surface chlorophyll-a penetrating fronts off the south coast of Java Island. *Deep Sea Research Part I: Oceanographic Research Papers,* 225. 104593. https://doi.org/10.1016/j.dsr.2025.104593.

Yun, C., Hwang, K., Han, S. & Ri, H. 2019. The effect of salinity stress on the biofuel production potential of freshwater microalgae chlorella vulgaris YH703. *Biomass and Bioenergy*, 127, 105277. https://doi.org/10.1016/j.biombioe.2019.105277.

Zampollo, A., Murray, R. O., Gallego, A. & Scott, B. 2025. Does the oceanographic response to wind farm wind-wakes affect the spring phytoplankton bloom?. *Progress in Oceanography,* 237, 103512. https://doi.org/10.1016/j.pocean.2025.103512.